

Spiking Wavelet Transformer

Yuetong Fang^{1*}, Ziqing Wang^{1*}, Lingfeng Zhang¹, Jiahang Cao¹, Honglei Chen¹,
and Renjing Xu^{1†}

The Hong Kong University of Science and Technology (Guangzhou), China *

Abstract. Spiking neural networks (SNNs) offer an energy-efficient alternative to conventional deep learning by mimicking the event-driven processing of the brain. Incorporating the Transformers with SNNs has shown promise for accuracy, yet it is incompetent to capture high-frequency patterns like moving edge and pixel-level brightness changes due to their reliance on global self-attention operations. Porting frequency representations in SNN is challenging yet crucial for event-driven vision. To address this issue, we propose the Spiking Wavelet Transformer (SWformer), an attention-free architecture that effectively learns comprehensive spatial-frequency features in a spike-driven manner by leveraging the sparse wavelet transform. The critical component is a Frequency-Aware Token Mixer (FATM) with three branches: 1) spiking wavelet learner for spatial-frequency domain learning, 2) convolution-based learner for spatial feature extraction, and 3) spiking pointwise convolution for cross-channel information aggregation. We also adopt negative spike dynamics to strengthen the frequency representation further. This enables the SWformer to outperform vanilla Spiking Transformers in capturing high-frequency visual components, as evidenced by our empirical results. Experiments on both static and neuromorphic datasets demonstrate SWformer’s effectiveness in capturing spatial-frequency patterns in a multiplication-free, event-driven fashion, outperforming state-of-the-art SNNs. SWformer achieves an over 50% reduction in energy consumption, a 21.1% reduction in parameter count, and a 2.40% performance improvement on the ImageNet dataset compared to vanilla Spiking Transformers.

Keywords: Spiking Neural Networks · Wavelet Transform · Vision Transformer · Event-based vision

1 Introduction

Spiking neural networks (SNNs) have gained considerable interest as a promising alternative to standard artificial neural networks (ANNs). Inspired by biological neurons, SNNs process visual information via binary events called spikes. Neurons transmit spikes only when their accumulated membrane potential exceeds a firing threshold, otherwise remaining inactive [60]. This sparse, event-driven processing offers orders of magnitude gains in efficiency and performance over conventional computing paradigms, especially on low-power neuromorphic chips, such as Loihi [10], True North [49], and Tianjic [56], which compute spikes asynchronously. With these advantages, there is a growing body of research applying SNNs across various areas, such as classification [31, 47, 71, 84], object detection [8, 67] and tracking [29, 72]. However, despite the

* * Equal Contribution; † Corresponding Author.

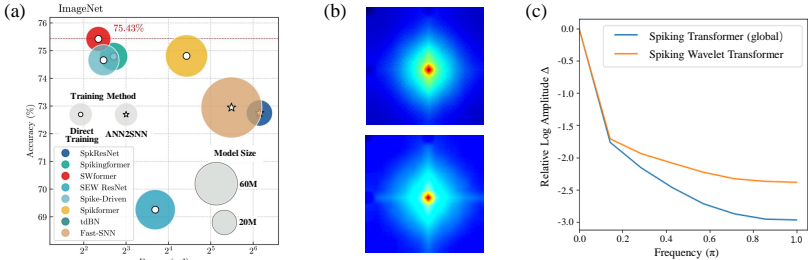


Fig. 1: (a) Performance of SWformer and other SOTA SNN models regarding top-1 accuracy, energy consumption, and parameter, with marker size reflecting the model size. (b) Fourier spectrum comparison between the Spiking Transformer with global attention [75] (top) and SWformer (bottom). (c) The corresponding relative log amplitudes of Fourier-transformed feature maps. (b-c) show that the SWformer captures more high-frequency signals, which leads to better performance.

remarkable energy efficiency of SNNs, they still lag behind ANNs in terms of accuracy, posing a major challenge.

To get the best of both worlds, a line of works focuses on incorporating advanced architectures from ANNs with the unique spiking mechanism in SNNs. This has led to notable developments. The introduction of residual learning into SNNs has facilitated the development of deeper network architectures and thus enhanced their performance [17, 26, 81]. More recently, integrating attention mechanisms has granted SNNs improved global information capturing, strengthening their capability to handle intricate patterns [73, 80]. This success has motivated researchers to discover the potential of combining powerful Transformer architecture with energy-efficient SNNs [75, 84]. While there has been some research in this direction, existing works mostly inherited the architecture from Vision Transformer [69], known to function solely in the spatial domain and exhibit similar characteristics of low-pass filters [54].

As a representative branch in neuromorphic computing, SNNs mimic biological vision by continuously sampling the input data and independently generating spikes in response to changes in the visual scene [25], conveying abundant local information. Specifically, neuromorphic data captures only brightness changes, primarily moving edges, which represent high-frequency patterns [40]. As supported by the empirical comparisons in **Fig. 1(b-c)**, though Spiking Transformers are highly capable of handling low-frequency components, like global shapes and structures, they are not very powerful for learning high-frequency information, mainly including abrupt changes in images such as local edges and textures [64] - this is intuitive since self-attention, their primary mechanism is a global operation that aggregates information across non-overlapping image patches. Porting the frequency information into SNNs is a natural and appealing idea; however, this has been non-trivial due to the spike-driven nature of SNNs.

Commonly used frequency analysis methods, like the Fourier transform, rely on precise matrix multiplications for data analysis [5]. In contrast, neurons in SNNs respond only to spike events - only a portion of spiking neurons are ever activated to execute sparse synaptic accumulation at any given time [10, 75]. This sparse, binary signaling

mechanism presents a significant obstacle in devising a spiking equivalent to measure the frequency features accurately. To reduce the information loss, existing works have investigated the adoption of precise data encoding like time-to-value mapping [43, 44], though at the expense of high latency. We argue that time-frequency decomposition can be a more effective and efficient representation space for SNNs, considering their sparse and robust properties [38]. In fact, the human visual system discerns elementary features through time-frequency components [19, 36]: it is found that the human visual system analyzes images in a way similar to the multi-resolution breakdown by the wavelet functions.

We thus propose the Spiking Wavelet Transformer (SWformer) to effectively capture time-frequency information in an event-driven manner. As shown in **Fig. 3**, SWformer integrates the sparse and computationally efficient merits of the wavelet transform with energy-efficient Spiking Transformers. As a result, SWformer captures more high-frequency information than Spiking Transformers with global attention, significantly enhancing performance, as observed in **Fig. 1**. SWformer enjoys multiplication-free, event-driven processing compatible with neuromorphic hardware while effectively capturing spatial-frequency information. The main contributions of this paper are:

- We propose Spiking Wavelet Transformer (SWformer), a novel attention-free architecture that integrates time-frequency information with Spiking Transformers to allow effective feature perception across a wide frequency range in a multiplication-free and event-driven manner.
- A key component of SWformer is the Frequency-Aware Token Mixer (FATM), which processes input in three branches to learn spatial, frequency, and cross-channel representations. This allows SWformer to capture more high-frequency visual information than vanilla spiking transformers.
- We incorporate negative spike dynamics, a simple yet effective approach to provide robust frequency representation in SNNs, from theoretical and experimental observation, .
- Extensive experiments demonstrate that our model significantly outperforms SOTA SNN performances, achieving a 2.95% improvement on static datasets like ImageNet and a remarkable 4% increase on neuromorphic datasets, such as CIFAR10-DVS.

2 Preliminary

2.1 Bio-inspired Spiking Neural Networks

Spiking Neural Networks (SNNs) can be considered as a variant of Artificial Neural Networks (ANNs) that mimic the spatial-temporal dynamics and binary spike activations found in biological neurons [60, 75]. This spike-based temporal processing paradigm allows sparse while efficient information transfer. However, the non-differentiable spike function hinders the use of gradient-based backpropagation for training SNNs effectively. Two main solutions exist: ANN-to-SNN conversion [6, 14] and direct training [48, 81]. The ANN-to-SNN conversion method aims to bridge the continuous activation value of ANNs with the firing rate of SNNs through neuron equivalence [6, 14], borrowing backpropagation to achieve high performance but requiring long simulation

timesteps and high energy consumption. In this work, we employ the direct training method to fully leverage the benefits of low-power and sparse event-driven computing of SNNs.

2.2 Neuromorphic Chips

Neuromorphic chips, inspired by the brain, merge processing and memory units, using spiking neurons and synapses as fundamental elements [60, 61]. As shown in **Fig. 2**, the synapse block processes incoming spikes, retrieves synaptic weights from memory, and generates spike messages to be routed to other cores [10, 49, 56]. This allows the energy-consuming Conv and MLP operations to be replaced by energy-efficient routing and sparse addition algorithms [11, 79], while self-attention is not yet supported. The spike-based computation grants neuromorphic chips high parallelism, scalability, and low power consumption (tens to hundreds of milliwatts) [2]. Our Spiking Wavelet Transformer design strictly adheres to the spike-driven paradigm, making it well-suited for implementation on neuromorphic chips.

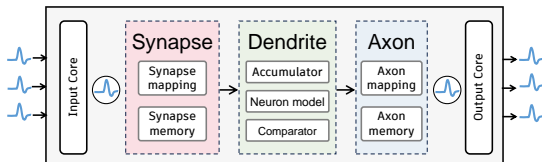


Fig. 2: Processing flow of a synapse block. Neuromorphic chips follow a spike-based computation paradigm, where both inputs and outputs are in spike form. [10]

2.3 Spiking Vision Transformers

Recent advancements in deep learning and neuroscience have concurrently propelled spiking neural networks (SNNs) [60]. Existing studies indicate that SNNs are particularly adept at incorporating brain-like processes such as long short-term memory [3, 57] and attention [74, 76]. Besides, deep learning techniques, particularly in network architecture, have enhanced the performance of SNNs while maintaining their unique spike-driven processing benefits. This has culminated in the development of Spiking Transformers [75, 83, 84], which merges the effectiveness of the Transformer model with the energy efficiency of SNNs, providing a solution for energy-sensitive scenarios [2]. However, previous works have directly inherited the Vision Transformer architecture [69], whose core self-attention mechanism primarily captures low-frequency information through global exchange among non-overlapping patch tokens, neglecting high-frequency components related to detailed information, local edges, and abrupt pixel-level changes [64]. Our work wants to emphasize the importance of high frequencies for Spiking Transformers, which is expected given the independent and sparse spike generation of SNNs that yields abundant high-frequency data cross layers.

2.4 Learning in the Frequency Domain

Frequency information is vital in image processing. Recent deep learning advancements incorporate frequency domain representations into Transformers, enhancing their ca-

pability to learn comprehensive features across a wide frequency range [21, 39, 77]. Integrating frequency representation into SNNs is particularly important, considering neuromorphic data reflects brightness changes corresponding to high frequencies. However, few works have applied frequency representation to SNNs, such as devising spiking band-pass filters [30] or neurons that spike at specific frequencies [1], struggling to capture full-frequency spectra. More recently, Lopez et.al [43, 44] adopted time-to-value mapping for accurate Fourier transform but at the cost of high latency (~ 1024 timesteps). In this work, we ingeniously combine the sparsity of wavelet transform with the binary and sparse signaling of SNNs to provide robust frequency representation.

3 Spiking Wavelet Transformer

We devise the Spiking Wavelet Transformer (SWformer), a new attention-free architecture that combines time-frequency information with Spiking Transformers. This allows for efficient feature perception across a wide frequency range without multiplication and in an event-driven manner. We will first briefly discuss the spiking neuron layer, followed by an overview of SWformer and its components.

The spiking neuron layer encodes spatio-temporal information into membrane potentials, converts them into binary spikes, and passes them on to the next layer for continued spike-based computation. Throughout this work, we consistently use the Leaky Integrate-and-Fire (LIF) neuron model [45], as it efficiently simulates biological neuron dynamics. The following equations govern the dynamics of the LIF layer:

$$U[n] = V[n - 1] + I[n], \quad (1)$$

$$s[n] = H(U[n] - V_{th}), \quad (2)$$

$$V[n] = V_{reset}s[n] + (\beta U[n])(1 - s[n]), \quad (3)$$

At each timestep n , the current membrane potential $U[n]$ is generated by integrating the spatial input $I[n]$, obtained from input data or intermediate operations like Conv and MLP, and temporal dynamics $V[n]$, which records the membrane potential’s evolution over time. If $U[n]$ exceeds the threshold V_{th} , the neuron fires a spike ($s[n]=1$), otherwise it remains inactive ($s[n]=0$). The Heaviside step function $H(\cdot)$ is used to determine the spiking behavior, where $H(x) = 1$ when $x \geq 0$. The temporal output $V[n]$ is updated based on the spiking activity and the decay factor β . The membrane potential $U[n]$ will decay to $V[n]$, if the neuron does not fire.

3.1 Overall Architecture

Fig. 3 presents SWformer, which comprises a Spiking Patch Splitting (SPS) module, Spiking Encoder blocks, and a linear classification head. The SPS module follows the design in [84]. For SNNs, the dimension of input sequence is $I \in \mathbb{R}^{T \times C \times H \times W}$, where T represents the number of timesteps. For static datasets, images are repeated T times to create a temporal sequence, while neuromorphic datasets inherently divide data into T frame sequences. For a 2D image sequence $I \in \mathbb{R}^{T \times C \times H \times W}$, the SPS is formulated as:

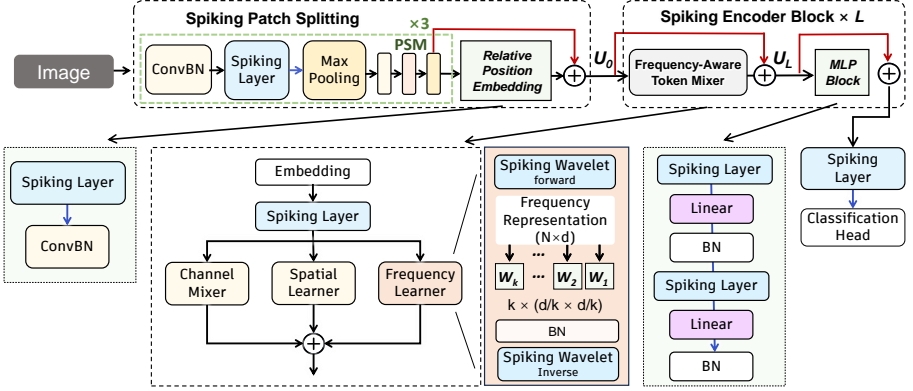


Fig. 3: The overview of Spike-driven Transformer. We introduce two key innovations to the network architecture from [84]. Firstly, FATM enhances Spiking Transformers’ frequency perception and only uses Conv and MLP operations, ensuring full compatibility with neuromorphic hardware. Secondly, our novel Frequency Learner utilizes spiking frequency representation to learn spectral features efficiently through block-diagonal multiplication. ConvBN denotes a convolution layer followed by a BN layer.

$$\begin{aligned}
 U &= \text{PSM}(I), & I &\in \mathbb{R}^{T \times C \times H \times W}, U \in \mathbb{R}^{T \times N \times D} \\
 s &= \text{Spk}(U), & s &\in \mathbb{R}^{T \times N \times D} \\
 \text{RPE} &= \text{ConvBN}(s), & \text{RPE} &\in \mathbb{R}^{T \times N \times D} \\
 U_0 &= U + \text{RPE}, & U_0 &\in \mathbb{R}^{T \times N \times D}
 \end{aligned} \tag{4}$$

where U and U_0 denotes output membrane potential tensor of PSM and SPS, respectively, with $\text{Spk}(\cdot)$ symbolizing the spiking neuron layer. The resulting patches are then processed by L Spiking Encoder Blocks, each consisting of a Frequency-Aware Token Mixer (FATM) followed by a Spiking MLP (S-MLP) block, with residual connections applied to output membrane potentials in both blocks. FATM enables multi-scale feature extraction based on the proposed spiking frequency representation (Sec. 3.3). The processed features from Spiking Encoders undergo Global Average-Pooling (GAP), resulting in a D -dimensional feature, which is then fed into a fully-connected Classification Head (CH) to produce the final prediction Y . The overall architecture of SWformer can be formulated as:

$$\begin{aligned}
 S_0 &= \text{Spk}(U_0), & S_0 &\in \mathbb{R}^{T \times N \times D} \\
 U_L &= \text{FATM}(S_{L-1}) + U_{L-1}, & U_L &\in \mathbb{R}^{T \times N \times D}, l = 1, \dots, M \\
 S_L &= \text{Spk}(\text{MLP}(\text{Spk}(U_L)) + U_L), & S_N &\in \mathbb{R}^{T \times N \times D} l = 1, \dots, M \\
 Y &= \text{CH}(\text{GAP}(S_N)),
 \end{aligned} \tag{5}$$

where U_L and S_L denotes the membrane potential and spike output of FATM at L -th layer, M refers to total number of layers.

3.2 Frequency-Aware Token Mixer

We propose the Frequency-Aware Token Mixer (FATM), a novel component designed to facilitate the mixing of tokens across a wide frequency range in SNNs. By integrating spiking frequency representation and convolution layers into Spiking Transformers, the FATM effectively captures and processes high-frequency information. As shown in **Fig. 3**, the FATM operates on all channels concurrently through three parallel branches: (1) Frequency Learner (FL): spiking wavelet learner that enables learning in the time-frequency domain, (2) Spatial Learner (SL): convolution-based learner that extracts spatial features, and (3) Channel Mixer (CM): spiking point-wise convolution that performs cross-channel information fusion. This design is inspired by the proven effectiveness of wavelet neural operators [68] and the local perception capability of the convolution operation. Moreover, we employ a block-diagonal structure to enhance computational parallelism and parameter efficiency by splitting the $d \times d$ weight matrix into k smaller matrices of size $d/k \times d/k$. By serving as an alternative to self-attention-based token mixers in Spiking Transformers [75, 83, 84], the FATM offers a powerful and efficient means of processing and mixing tokens in the frequency spectrum. Technically, for an input feature sequence $S_L \in \mathbb{R}^{T \times N \times D}$, the FATM can be expressed as follows:

$$\begin{aligned}
 S_L &\rightarrow S'_L & S'_L &\in \mathbb{R}^{T \times k \times N/k \times H \times W}, l = 1, \dots, M \\
 U_{FL} &= FL(S_L) & U_{Freq} &\in \mathbb{R}^{T \times N \times D}, l = 1, \dots, M \\
 U'_{SL} &= ConvBN(S'_L) & U'_{SL} &\in \mathbb{R}^{T \times k \times N/k \times H \times W}, l = 1, \dots, M \\
 U'_{CM} &= ConvBN(S'_L) & U'_{CM} &\in \mathbb{R}^{T \times k \times N/k \times H \times W}, l = 1, \dots, M \\
 U_{SL} &\rightarrow U_{SL} & U_{SL} &\in \mathbb{R}^{T \times N \times D} \\
 U_{CM} &\rightarrow U_{CM} & U_{CM} &\in \mathbb{R}^{T \times N \times D} \\
 U_{FATM} &= U_{FL} + U_{SL} + U_{CM} & U_{FATM} &\in \mathbb{R}^{T \times N \times D}
 \end{aligned} \tag{6}$$

where U_{FL} , U'_{SL} , U'_{CM} , represent the membrane potential outputs of the Frequency Learner, Spatial Learner, and Channel Mixer, respectively, while \rightarrow denotes the reshape operation. The Spatial Learner and Channel Mixer incorporate 3×3 and 1×1 convolutions, respectively, leveraging the powerful capabilities of CNNs to enhance the learning of local features.

3.3 Frequency Learner

The Frequency Learner projects features to a transform domain, weighting and passing specific frequency modes. It incorporates two key designs: a robust spiking frequency representation that links the sparsity of wavelet transform with SNN's binary and sparse signaling property, and a modularized weight matrix that enhances parameter efficiency and computational parallelism.

Frequency representation in SNNs elegantly addresses the challenges of incorporating spike-driven frequency information in SNNs. Our approach is motivated by two key insights: (1) the unique spiking output and reset behavior of neuromorphic chips, as shown in **Fig. 2**, necessitates the conversion of intermediate results to spikes, which complicates the direct adoption of signal transform algorithms involving cascaded matrix multiplications; and (2) the amplitude-dependent response of spiking

neurons makes algorithms with complex number operations, like the Fourier Transform, resource-intensive, as they require separate neuron banks for handling real and complex-valued computations.

We devise the spiking frequency representation adopting wavelet transform, as it naturally complements the sparse signaling of SNNs. This intuitive combination allows us to capture both high-frequency details and low-frequency approximations using a sparse representation, while the decorrelation property of wavelet transform adds robustness to signal transfer. In this work, we specifically adopt the Haar transform, the simplest type of wavelet transform, which uses a square-shaped mother wavelet function. Basically, the spiking Haar forward and inverse transform can be formulated as:

$$\begin{aligned} Haar_{\text{forward}} &= Spk(W_{\text{haar}} \cdot Spk(I \cdot W_{\text{haar}}^{\top})) \\ I &= Spk(W_{\text{haar}}^{\top} \cdot Spk(Haar_{\text{forward}} \cdot W_{\text{haar}})) \end{aligned} \quad (7)$$

$$\begin{aligned} W_{\text{haar}}(1) &= [1], \\ W_{\text{haar}}(n) &= \frac{1}{\sqrt{2}} \begin{bmatrix} W_{\text{haar}}(n-1) \otimes [1, 1] \\ I_{2^{n-1}} \otimes [1, -1] \end{bmatrix}, \quad \text{for } n > 1 \end{aligned} \quad (8)$$

where I and $Haar_{\text{forward}}$ represent the raw input and the matrix after Haar forward transform, respectively, and W_{haar} denotes the transformation matrix. Ideally, the Haar inverse transform can recover $Haar_{\text{forward}}$ back to I without any error.

However, binary SNNs only generate $\{0, 1\}$ spikes, while Eq. (8) shows that the Haar transform involves negative terms, leading to significant errors. To resolve this issue, we incorporate negative spike dynamics, supported by neuromorphic chips [10, 58], expanding the spike values to $\{-1, 0, 1\}$. The ternary neuron model can be expressed as:

$$U[n] = V[n-1] + I[n], \quad (9)$$

$$s[n] = H_{\text{sym}}(U[n-1], V_{\text{th}}), \quad (10)$$

$$V[n] = V_{\text{reset}}s[n] + U[n](1 - s[n]), \quad (11)$$

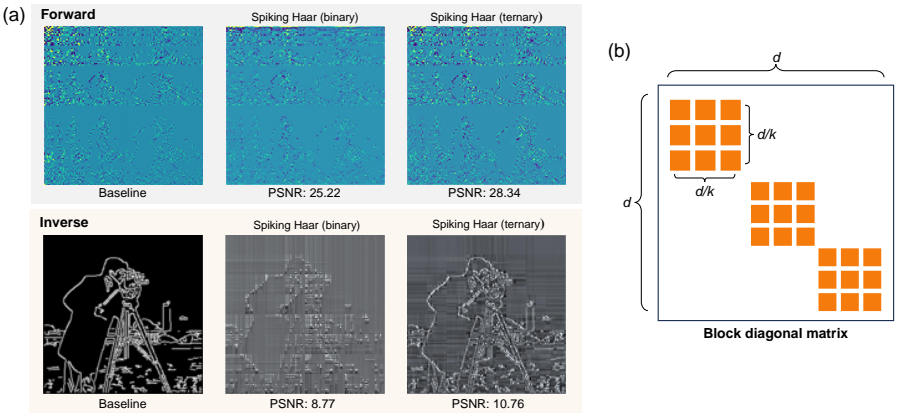


Fig. 4: (a) Comparative analysis of the standard Haar transform, binary spiking Haar transform, and ternary spiking Haar transform. Higher Peak Signal-to-Noise Ratio (PSNR) values indicate greater similarity between the images. (b) Schematic of block-diagonal matrix.

where $H_{sym}(\cdot)$ refers to a symmetric Heaviside step function, defined as $H_{sym}(x) = 1$ when $x \geq 1$, and $H_{sym}(x) = -1$ when $x \leq -1$. Here, we adopt the integrate-and-fire neuron [7], equivalent to the LIF neuron with $\beta = 1$, to ensure accurate signal transformation. As demonstrated in Fig. 4, the incorporation of negative spike dynamics significantly enhances the quality of the spiking frequency representation. The spiking frequency representation, also known as spiking wavelet transform in this article, consists of forward and inverse transform process.

Modularized Weight Matrix enables interpretability, computational parallelization, and parameter efficiency, which can be interpreted as batch matrix multiplication [9]. As illustrated in Fig. 4(b), the block-diagonal multiplication approach divides the $d \times d$ weight matrix into k smaller weight blocks, each having a size of $d/k \times d/k$. This technique effectively reduces the parameter count from $O(d^2)$ to $O(d^2/k)$, with better parallelism. With this structure in place, the Frequency Learner independently processes each splitting block as follows:

$$\tilde{y}_{m,n}^{\ell} = W_{m,n}^{\ell} x_{m,n}^{\ell}, \quad \ell = 1, \dots, k, (m, n) \in H \times W \quad (12)$$

where m, n refers to the spatial coordinates of a token within the input tensor, and ℓ denotes the corresponding block id. Thus, each block can be understood as a head in a multi-head self-attention mechanism, projecting the data into a specific subspace. To capture meaningful information in each subspace, it is essential to choose an appropriate number of splitting blocks that allows for a sufficiently high-dimensional representation. This enables efficient feature extraction in the frequency spectrum.

3.4 Membrane Shortcut

Residual learning and shortcuts have emerged as crucial techniques for training deep SNNs [18, 24, 28, 82]. These techniques focus on two primary principles. First, they aim to implement identity mapping to alleviate the degradation problem that can occur in deep networks [24]. Second, they strive to maintain spike-driven computing, which is crucial for hardware compatibility and forms the foundation of SNN's energy efficiency. As shown in Fig. 5, there are three mainstream shortcut techniques commonly employed in SNNs. Vanilla Shortcut scheme [82] directly borrows the shortcut scheme from ANN [23], establishing a shortcut connection between membrane potential and spike. While it ensures spike-driven processing, it cannot impose identity

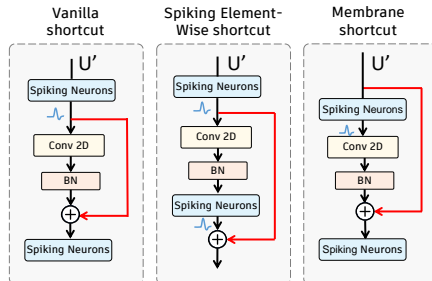


Fig. 5: Mainstream shortcut schemes in SNNs.

mapping [24]. The Spiking Element-Wise Shortcut [18] creates a shortcut path to connect spikes across different layers. However, this scheme operates in an "integer-driven" manner rather than a "spike-driven" one, as the output spike addition results in integral values. On the other hand, the Membrane Shortcut [28] offers the benefits of both identity mapping and spike-driven computation. This method forms a shortcut between the membrane potentials of spiking neurons in separate layers, which can be understood as an approach to optimize the membrane potential distribution. This technique has been adopted in recent Spiking Transformer [75]. Our SWformer harnesses the membrane shortcut to leverage its biological plausibility and high-performance advantage [28, 75].

4 Experiment

4.1 Experiment Setup

Spiking Neural Networks (SNNs) are spatio-temporal dynamic networks that naturally handle temporal tasks. For static image classification, it is common practice to repeatedly input the same image at each timestep. While increasing simulation timesteps can improve accuracy, it also increases training time, hardware requirements, and inference energy consumption. Neuromorphic datasets with inherent spatio-temporal dynamics can fully exploit the energy-efficient advantages of SNNs.

Dataset We evaluate our approach on a range of datasets, including static datasets like CIFAR-10 [34], CIFAR-100 [33], and ImageNet [12], as well as neuromorphic datasets such as CIFAR10-DVS [37], N-Caltech101 [52], N-Cars [65], ActionRecognition [51], ASL-DVS [4], and NavGesture [46] datasets.

Training settings We implement the SWformer model based on PyTorch [55] and SpikingJelly [16]. To estimate the theoretical energy consumption of SWformer, we follow the approach in previous studies [26, 53, 75, 78, 84], estimating the theoretical energy consumption by measuring the synaptic operations (SOPs) [50]. Training is conducted on 8 NVIDIA A800 GPUs. The Supplementary Material provides details on energy consumption evaluation and implementation.

4.2 Performance on Static Datasets

ImageNet SWformer, our proposed model, outperforms the vanilla Spiking Transformer (SpikFormer) and other ResNet-based SNNs on ImageNet in terms of accuracy and power efficiency. Experiments with different embedding dimensions, transformer blocks, and spiking wavelet settings demonstrate the importance of precise frequency information as shown in **Table 1**. SWformer (Block=2) with the Transformer-6-512 setting achieves 74.98% accuracy, 2.52% higher than SpikFormer, while reducing power consumption by 61.9% ($V_{th}=0.5$). Increasing the number of splitting blocks further improves parameter efficiency and power consumption without compromising accuracy. Specifically, SWformer 6-512-block2- V_{th} 0.5 reaches 74.98% accuracy with 21.8M parameters, surpassing MS-ResNet-34 [27] and SEW-ResNet-34 [17], which achieve 67.04% and 69.15% accuracy, respectively, with approximately 21.8M parameters. Note that the baseline using standard wavelet transform, shown in gray, generally achieves better performance, highlighting the importance of accurate frequency representation in SNNs, despite contradicting the spike-driven computing paradigm. To fully leverage the energy efficiency benefits of neuromorphic computing, specific hardware design for frequency domain processing is worth investigating.

Table 1: Performance comparison between the proposed model and the SOTA models on the ImageNet dataset. Models denoted with an asterisk (*) use an input resolution of 256×256 , which is essential for the Haar transform to achieve optimal performance and consistent application throughout the entire input. All models were trained for 310 epochs with identical initial settings for a fair comparison. †: B denotes the number of splitting blocks. —: standard wavelet transform.

Methods	Architecture	# Param (M)	Power (mJ)	Time Steps	Accuracy (%)	
Hybrid training [59] ^{ICLR}	ResNet-34	21.79	-	250	61.48	
	SEW-ResNet-34	21.79	4.04	4	67.04	
SEW ResNet [18] ^{NeurIPS}	SEW-ResNet-50	25.56	4.89	4	67.78	
	SEW-ResNet-101	44.55	8.91	4	68.76	
	SEW-ResNet-152	60.19	12.89	4	69.26	
	TET [13] ^{ICLR}	SEW-ResNet-34	21.79	-	4	68.00
MS ResNet [27] ^{TNNLS}	MS-ResNet-18	11.69	4.29	4	63.10	
	MS-ResNet-34	21.80	5.11	4	69.42	
Spiking ResNet [26] ^{TNNLS}	ResNet-50	25.56	70.93	350	72.75	
tdBN [81] ^{AAAI}	Spiking-ResNet-34	21.79	6.39	6	63.72	
ANN Transformer*	Transformer-6-512	23.37	40.72	-	80.54	
SpikFormer [84] ^{ICLR}	Transformer-8-384	16.81	7.73	4	70.24	
	Transformer-6-512	23.37	9.41	4	72.46	
	Transformer-8-512	29.68	11.57	4	73.38	
SWfomer* (B [†] =2)	—	Transformer-6-512	21.8(-7%)	4.00(-57.4%)	4	75.09(+2.63)
	—	Transformer-8-512	27.6(-7%)	4.31(-62.7%)	4	75.26(+1.88)
	Vth=0.5	Transformer-6-512	21.8	3.58(-61.9%)	4	74.98(+2.52)
		Transformer-8-512	27.6	4.89(-57.7%)	4	75.18(+1.80)
	Vth=1	Transformer-6-512	21.8	3.87(-58.8%)	4	74.84(+2.38)
		Transformer-8-512	27.6	5.08(-56.1%)	4	75.43(+2.05)
SWfomer* (B [†] =4)	—	Transformer-6-512	18.46(-21%)	3.51(-62.7%)	4	74.86(+2.40)
	—	Transformer-8-512	23.14(-22%)	4.67(-59.6%)	4	75.33(+1.95)
	Vth=0.5	Transformer-6-512	18.46	3.91(-58.4%)	4	74.62(+2.16)
		Transformer-8-512	23.14	4.98(-57.0%)	4	75.08(+1.7)
	Vth=1	Transformer-6-512	18.46	3.75(-60.1%)	4	74.69(+2.23)
		Transformer-8-512	23.14	4.87(-57.9%)	4	75.29(+1.91)

CIFAR10/ CIFAR100 Table 2 presents a comprehensive comparison of the MST model with current state-of-the-art SNN models on the CIFAR-10/100. SWfomer outperforms all other models in terms of top-1 accuracy on both datasets with fewer parameters and time steps. In specific, compared to ResNet-based SNN models like tdBN [81], our SWfomer model outperforms it by **2.0%** on CIFAR10 and **5.4%** on CIFAR100, with only **59.5%** of the parameters. Additionally, the SWfomer model also surpasses Transformer-based SNNs in accuracy and parameter efficiency. The superior performance of SWfomer can be attributed to its unique designs.

Discussion By incorporating spiking dynamics and wavelet-based frequency analysis, SWfomer can efficiently process and represent information in a more biologically plausible manner. The combination of these two powerful techniques enables SWfomer to capture both spatial, temporal and frequency dependencies in the input data, leading to improved accuracy and power efficiency compared to vanilla Spiking Transformers and ResNet-based SNNs. Furthermore, the modular architecture of SWfomer allows for flexible scaling and customization, making it adaptable to various tasks and resource constraints.

Table 2: Performance comparison on CIFAR10/ CIFAR100 and CIFAR10-DVS Datasets.

Method	CIFAR10			CIFAR100			CIFAR10-DVS		
	# Param (M)	T	Acc. (%)	# Param (M)	T	Acc. (%)	# Param (M)	T	Acc. (%)
TET [13] ^{ICLR}	12.63	6	94.50	12.63	6	74.72	9.27	10	83.32
tdBN [81] ^{AAAI}	12.63	4	92.92	12.63	4	70.86	12.63	10	67.8
TEBN [15] ^{NeurIPS}	12.63	6	94.71	12.63	6	76.41	-	10	75.10
Real Spike [22] ^{ECCV}	12.63	6	95.78	39.9	10	71.24	12.63	10	72.85
DSR [47] ^{CVPR}	11.2	20	95.4	11.2	20	78.5	9.48	10	77.51
SpikFormer [84] ^{ICLR}	9.32	4	95.51	9.32	4	78.21	2.59	10	78.9
	9.32	6	95.34	9.32	4	78.61	2.59	16	80.9
SWformer (Ours)	7.51	4	96.1(+0.59)	7.51	4	79.3(+0.9)	2.05	10	82.9(+4.0)
	7.51	6	96.3(+0.96)	7.51	6	79.6(+1.0)	2.05	16	83.9(+3.0)

Table 3: Performance of our proposed model versus SOTA models on various neuromorphic datasets.

Datasets	Methods	T	Acc. (%)
N-CALTECH101	SALT [32]	20	55.00
	TCJA [85]	14	78.50
	TIM [63]	10	79.00
	TT-SNN [35]	6	77.00
	NDA [41]	10	83.70
	SWformer (ours)	10	88.45
N-CARS	CarSNN [70]	10	86.00
	NDA [41]	10	91.90
	SWformer (ours)	10	96.32
Action Recognition	STCA [20]	10	71.20
	Mb-SNN [42]	10	78.10
	SWformer (ours)	10	88.88
ASL-DVS	Meta-SNN [66]	100	96.04
	SWformer (ours)	10	99.88
NavGesture	KNN [46]	-	95.90
	SWformer (ours)	10	98.49

Table 4: Ablation study on Frequency Aware Token Mixer

Datasets	Models	T	Acc. (%)
CIFAR100	SWformer-4-384 _{NoHaar}	4	78.89
	SWformer-4-384 _{MaskDC}	4	79.34
	SWformer-4-384 _{NoNeg}	4	78.64
	SWformer-4-384 _{NoInv}	4	78.79
	SWformer-4-384 _{base}	4	79.31
CIFAR10-DVS	SWformer-2-256 _{NoHaar}	16	79.9
	SWformer-2-256 _{MaskDC}	16	84.0
	SWformer-2-256 _{NoPool}	16	81.8
	SWformer-2-256 _{base}	16	83.9

4.3 Performance on Neuromorphic Datasets

As shown in **Table 2** and **Table 3**, the proposed SWformer outperforms state-of-the-art (SOTA) SNN models on a variety of neuromorphic datasets, including CIFAR10-DVS [37], N-Caltech101 [52], and N-Cars [65], which are derived from static datasets and converted into neuromorphic data using event-based cameras. To further enhance high-frequency information in these datasets, a 1D max-pooling layer is placed at the beginning of the FATM module. SWformer achieves impressive accuracy on all neuromorphic tasks. These results surpass previous SOTA models by significant margins, with SWformer outperforming NDA [41] by 4.75% and 4.42% on N-CALTECH101 and N-CARS, Mb-SNN [42] by 10.78% on Action Recognition, Meta-SNN [66] by 3.84% while using 10 times fewer timesteps on ASL-DVS, and KNN [46] by 2.59% on NavGesture.

Discussion The effectiveness and superiority of the SWformer model compared to existing SOTA SNN models across a wide range of neuromorphic datasets are clearly demonstrated by these results. SWformer’s design, which explicitly incorporates feature learning in the frequency spectrum, is highly effective at capturing the abundant high-frequency components in neuromorphic datasets, strongly supporting the insights behind its development.

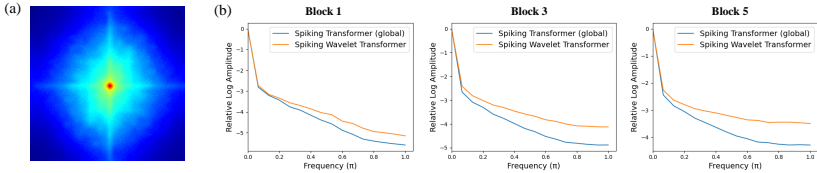


Fig. 6: (a) Fourier-transformed feature map of SPS output. (b) Relative log amplitudes of Fourier-transformed feature maps from model blocks 1, 3, and 5.

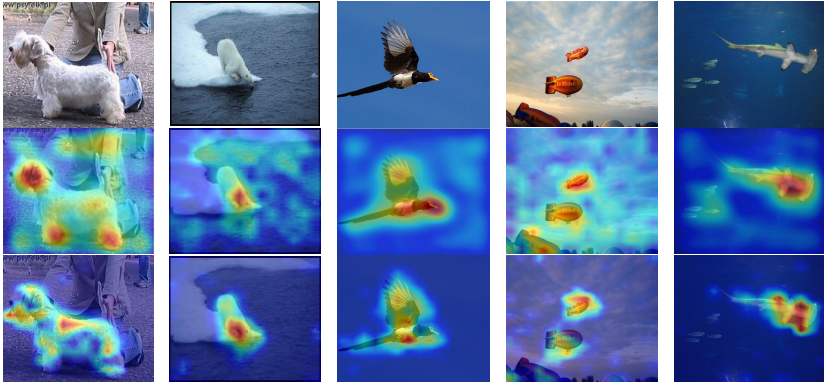


Fig. 7: Grad-CAM [62] activation map visualization of the original inputs (top), the global Spiking Self-Attention block in Spiking Transformer [75] (middle), and the Frequency-Aware Token Mixer in SWformer (bottom).

4.4 Method Analysis

Visualization Existing Spiking Transformers [75, 83, 84] adopt the vanilla Transformer [69] design, using global operations to exchange information among non-overlapping patch tokens. However, SNNs generate output activation maps rich in high-frequency components. As illustrated in **Fig. 6(a)**, data processed by the Spiking Patch Splitting (SPS) module, the initial embedding operation before the visual data is processed by Transformer blocks, contains information across a wide frequency range. In contrast, our SWformer’s FATM effectively captures specific frequency information on the corresponding channel, enabling comprehensive feature learning in the frequency spectrum and maintaining high-frequency information transmission even in deeper layers (**Fig. 6(b)**). This enhanced frequency learning capability facilitates more accurate and complete frequency feature learning and object location, as shown in **Fig. 7**, leading to improved object recognition capability and overall performance.

Number of Splitting Blocks An appropriate number of splitting blocks in SWformer can lead to a more efficient architecture that strikes a better balance between performance and resource utilization. As shown in **Fig. 4(b)**, increasing the number of splitting blocks directly reduce the number of parameters. This relationship is further explored in **Table 1**, which demonstrates that by increasing the splitting blocks from 2 to 4 in SWformer, both the number of parameters and power consumption can be reduced while still maintaining high accuracy. Specifically, SWformer (Block=4) has about 21% fewer parameters than SWformer (Block=2) for both Transformer-6-512 and Transformer-8-512 architectures. Despite the reduced resources, SWformer (Block=4)

achieves accuracy improvements of 2.16% to 2.40% for Transformer-6-512 and 1.70% to 1.95% for Transformer-8-512 compared to SpikFormer. These findings highlight the importance of the appropriate number of splitting blocks in SWformer to create a more efficient architecture without compromising performance.

Firing Threshold of Spiking Frequency Representation Spiking neurons act as temporal pruning for inputs, leading to better energy efficiency. As shown in Fig. 4 and Table 1, the inherent sparsity and robustness of the wavelet transform allow for a significant reduction in power consumption without compromising accuracy. Increasing the V_{th} in SWformer (Block=4) reduces power consumption by 58.4% to 60.1%. This effect depends on the specific V_{th} value and Transformer architecture. Besides, the baseline using standard wavelet transform, without inserted spiking layers, represented by the gray background data, generally achieves better performance, emphasizing the importance of precise frequency representation in SNNs, albeit contradicting the spike-driven computing paradigm. Therefore, our spiking frequency representation, which combines wavelet transform with SNNs, is crucial for the entire model design, enabling robust signal projection in just 4 timesteps, as shown in Fig. 4.

Ablation Study of Frequency-Aware Token Mixer To better understand the advantages of the Frequency-Aware Token Mixer (FATM), we performed ablation studies. Removing spiking wavelet transforms significantly decreased performance on CIFAR100 and CIFAR10-DVS, highlighting the critical role of frequency feature learning. Interestingly, masking the DC components actually improves performance, highlighting the significance of high-frequency information. Furthermore, when processing the CIFAR10-DVS dataset, removing the 1D max-pooling operation leads to a performance drop from 83.9% to 81.8%. We also assessed the effectiveness of the spiking frequency representation. Evaluating CIFAR100 without negative spike dynamics and spiking Haar inverse transform results in performance reductions from 79.31% to 78.64% and 78.79%, respectively. These findings underscore the vital importance of accurate frequency representation in FATM for achieving optimal performance and emphasize the crucial role of high-frequency components SNNs.

5 Conclusion

In this work, we develop the Spiking Wavelet Transformer (SWformer), a powerful alternative to self-attention-based token mixers, with promising performance and parameter efficiency. The core innovation of SWformer is its Frequency-Aware Token Mixer (FATM), which combines spatial, frequency, and channel mixing branches. This unique design enables SWformer to emphasize high-frequency components and enhance the perception capability of Spiking Transformers in the frequency spectrum. Furthermore, we introduce a novel spiking frequency representation that facilitates robust, multiplication-free, and event-driven signal transform. Extensive experiments show that SWformer surpasses representative SNNs on both static and neuromorphic datasets, underscoring the crucial role of frequency learning in spiking neural networks. We believe this study offers the community valuable insights for designing efficient and effective SNN architectures.

References

1. Auge, D., Mueller, E.: Resonate-and-fire neurons as frequency selective input encoders for spiking neural networks (2020)
2. Basu, A., Deng, L., Frenkel, C., Zhang, X.: Spiking neural network integrated circuits: A review of trends and future directions. In: 2022 IEEE Custom Integrated Circuits Conference (CICC). pp. 1–8. IEEE (2022)
3. Bellec, G., Salaj, D., Subramoney, A., Legenstein, R., Maass, W.: Long short-term memory and learning-to-learn in networks of spiking neurons. *Advances in neural information processing systems* **31** (2018)
4. Bi, Y., Chadha, A., Abbas, A., Bourtsoulatzé, E., Andreopoulos, Y.: Graph-based object classification for neuromorphic vision sensing. In: Proceedings of the IEEE/CVF International Conference on Computer Vision. pp. 491–501 (2019)
5. Bochner, S., Chandrasekharan, K.: Fourier transforms. No. 19, Princeton University Press (1949)
6. Bu, T., Fang, W., Ding, J., Dai, P., Yu, Z., Huang, T.: Optimal ANN-SNN Conversion for High-accuracy and Ultra-low-latency Spiking Neural Networks. In: International Conference on Learning Representations (2021)
7. Burkitt, A.N.: A review of the integrate-and-fire neuron model: I. homogeneous synaptic input. *Biological cybernetics* **95**, 1–19 (2006)
8. Cao, Y., Chen, Y., Khosla, D.: Spiking deep convolutional neural networks for energy-efficient object recognition. *International Journal of Computer Vision* **113**(1), 54–66 (2015)
9. Dao, T., Chen, B., Sohoni, N.S., Desai, A., Poli, M., Grogan, J., Liu, A., Rao, A., Rudra, A., Ré, C.: Monarch: Expressive structured matrices for efficient and accurate training. In: International Conference on Machine Learning. pp. 4690–4721. PMLR (2022)
10. Davies, M., Srinivasa, N., Lin, T.H., Chinya, G., Cao, Y., Choday, S.H., Dimou, G., Joshi, P., Imam, N., Jain, S., et al.: Loihi: A neuromorphic manycore processor with on-chip learning. *Ieee Micro* **38**(1), 82–99 (2018)
11. Davies, M., Wild, A., Orchard, G., Sandamirskaya, Y., Guerra, G.A.F., Joshi, P., Plank, P., Risbud, S.R.: Advancing neuromorphic computing with loihi: A survey of results and outlook. *Proceedings of the IEEE* **109**(5), 911–934 (2021)
12. Deng, J., Dong, W., Socher, R., Li, L.J., Li, K., Fei-Fei, L.: Imagenet: A large-scale hierarchical image database. In: 2009 IEEE Conference on Computer Vision and Pattern Recognition. pp. 248–255. Ieee (2009)
13. Deng, S., Li, Y., Zhang, S., Gu, S.: Temporal efficient training of spiking neural network via gradient re-weighting. arXiv preprint arXiv:2202.11946 (2022)
14. Ding, J., Yu, Z., Tian, Y., Huang, T.: Optimal ann-snn conversion for fast and accurate inference in deep spiking neural networks. arXiv preprint arXiv:2105.11654 (2021)
15. Duan, C., Ding, J., Chen, S., Yu, Z., Huang, T.: Temporal effective batch normalization in spiking neural networks. *Advances in Neural Information Processing Systems* **35**, 34377–34390 (2022)
16. Fang, W., Chen, Y., Ding, J., Yu, Z., Masquelier, T., Chen, D., Huang, L., Zhou, H., Li, G., Tian, Y.: Spikingjelly: An open-source machine learning infrastructure platform for spike-based intelligence. *Science Advances* **9**(40), eadi1480 (2023)
17. Fang, W., Yu, Z., Chen, Y., Huang, T., Masquelier, T., Tian, Y.: Deep residual learning in spiking neural networks. *Advances in Neural Information Processing Systems* **34**, 21056–21069 (2021)
18. Fang, W., Yu, Z., Chen, Y., Huang, T., Masquelier, T., Tian, Y.: Deep residual learning in spiking neural networks. *Advances in Neural Information Processing Systems* **34**, 21056–21069 (2021)

19. Gaudart, L., Crebassa, J., Petrakian, J.P.: Wavelet transform in human visual channels. *Appl. Opt.* **32**(22), 4119–4127 (Aug 1993). <https://doi.org/10.1364/AO.32.004119>, <https://opg.optica.org/ao/abstract.cfm?URI=ao-32-22-4119>
20. Gu, P., Xiao, R., Pan, G., Tang, H.: STCA: Spatio-Temporal Credit Assignment with Delayed Feedback in Deep Spiking Neural Networks. In: *Proceedings of the Twenty-Eighth International Joint Conference on Artificial Intelligence*. pp. 1366–1372. International Joint Conferences on Artificial Intelligence Organization, Macao, China (Aug 2019). <https://doi.org/10.24963/ijcai.2019/189>
21. Guibas, J., Mardani, M., Li, Z., Tao, A., Anandkumar, A., Catanzaro, B.: Efficient token mixing for transformers via adaptive fourier neural operators. In: *International Conference on Learning Representations* (2021)
22. Guo, Y., Zhang, L., Chen, Y., Tong, X., Liu, X., Wang, Y., Huang, X., Ma, Z.: Real spike: Learning real-valued spikes for spiking neural networks. In: *European Conference on Computer Vision*. pp. 52–68. Springer (2022)
23. He, K., Zhang, X., Ren, S., Sun, J.: Deep residual learning for image recognition. In: *Proceedings of the IEEE conference on computer vision and pattern recognition*. pp. 770–778 (2016)
24. He, K., Zhang, X., Ren, S., Sun, J.: Identity mappings in deep residual networks. In: *Computer Vision–ECCV 2016: 14th European Conference, Amsterdam, The Netherlands, October 11–14, 2016, Proceedings, Part IV* 14. pp. 630–645. Springer (2016)
25. Hopkins, M., Pineda-Garcia, G., Bogdan, P.A., Furber, S.B.: Spiking neural networks for computer vision. *Interface Focus* **8**(4), 20180007 (2018)
26. Hu, Y., Tang, H., Pan, G.: Spiking deep residual networks. *IEEE Transactions on Neural Networks and Learning Systems* (2021)
27. Hu, Y., Deng, L., Wu, Y., Yao, M., Li, G.: Advancing spiking neural networks towards deep residual learning. *arXiv preprint arXiv:2112.08954* (2021)
28. Hu, Y., Deng, L., Wu, Y., Yao, M., Li, G.: Advancing spiking neural networks toward deep residual learning. *IEEE Transactions on Neural Networks and Learning Systems* (2024)
29. Ji, M., Wang, Z., Yan, R., Liu, Q., Xu, S., Tang, H.: Sctn: Event-based object tracking with energy-efficient deep convolutional spiking neural networks. *Frontiers in Neuroscience* **17**, 1123698 (2023)
30. Jiménez-Fernández, A., Cerezuela-Escudero, E., Miró-Amarante, L., Domínguez-Morales, M.J., de Asís Gómez-Rodríguez, F., Linares-Barranco, A., Jiménez-Moreno, G.: A binaural neuromorphic auditory sensor for fpga: a spike signal processing approach. *IEEE transactions on neural networks and learning systems* **28**(4), 804–818 (2016)
31. Kim, Y., Panda, P.: Optimizing deeper spiking neural networks for dynamic vision sensing. *Neural Networks* **144**, 686–698 (2021)
32. Kim, Y., Panda, P.: Optimizing deeper spiking neural networks for dynamic vision sensing. *Neural Networks* **144**, 686–698 (2021)
33. Krizhevsky, A., Hinton, G.: Learning multiple layers of features from tiny images (2009)
34. Lecun, Y., Bottou, L., Bengio, Y., Haffner, P.: Gradient-based learning applied to document recognition. *Proceedings of the IEEE* **86**(11), 2278–2324 (Nov 1998). <https://doi.org/10.1109/5.726791>
35. Lee, D., Yin, R., Kim, Y., Moitra, A., Li, Y., Panda, P.: Tt-snn: Tensor train decomposition for efficient spiking neural network training. *arXiv preprint arXiv:2401.08001* (2024)
36. Lee, I., Kim, J., Kim, Y., Kim, S., Park, G., Park, K.T.: Wavelet transform image coding using human visual system. In: *Proceedings of APCCAS'94-1994 Asia Pacific Conference on Circuits and Systems*. pp. 619–623. IEEE (1994)
37. Li, H., Liu, H., Ji, X., Li, G., Shi, L.: CIFAR10-DVS: An Event-Stream Dataset for Object Classification. *Frontiers in Neuroscience* **11** (2017)

38. Li, Q., Shen, L., Guo, S., Lai, Z.: Wavelet integrated cnns for noise-robust image classification. In: Proceedings of the IEEE/CVF Conference on Computer Vision and Pattern Recognition. pp. 7245–7254 (2020)
39. Li, X., Zhang, Y., Yuan, J., Lu, H., Zhu, Y.: Discrete cosin transformer: Image modeling from frequency domain. In: Proceedings of the IEEE/CVF Winter Conference on Applications of Computer Vision. pp. 5468–5478 (2023)
40. Li, Y., Kim, Y., Park, H., Geller, T., Panda, P.: Neuromorphic data augmentation for training spiking neural networks. In: European Conference on Computer Vision. pp. 631–649. Springer (2022)
41. Li, Y., Kim, Y., Park, H., Geller, T., Panda, P.: Neuromorphic Data Augmentation for Training Spiking Neural Networks. arXiv preprint arXiv:2203.06145 (2022)
42. Liu, Q., Xing, D., Tang, H., Ma, D., Pan, G.: Event-based Action Recognition Using Motion Information and Spiking Neural Networks. In: Proceedings of the Thirtieth International Joint Conference on Artificial Intelligence. pp. 1743–1749. International Joint Conferences on Artificial Intelligence Organization, Montreal, Canada (Aug 2021). <https://doi.org/10.24963/ijcai.2021/240>
43. López-Randulfe, J., Duswald, T., Bing, Z., Knoll, A.: Spiking neural network for fourier transform and object detection for automotive radar. *Frontiers in Neurorobotics* **15**, 688344 (2021)
44. López-Randulfe, J., Reeb, N., Karimi, N., Liu, C., Gonzalez, H.A., Dietrich, R., Vogginger, B., Mayr, C., Knoll, A.: Time-coded spiking fourier transform in neuromorphic hardware. *IEEE Transactions on Computers* **71**(11), 2792–2802 (2022)
45. Maass, W.: Networks of spiking neurons: the third generation of neural network models. *Neural networks* **10**(9), 1659–1671 (1997)
46. Maro, J.M., Ieng, S.H., Benosman, R.: Event-based gesture recognition with dynamic background suppression using smartphone computational capabilities. *Frontiers in neuroscience* **14**, 275 (2020)
47. Meng, Q., Xiao, M., Yan, S., Wang, Y., Lin, Z., Luo, Z.Q.: Training High-Performance Low-Latency Spiking Neural Networks by Differentiation on Spike Representation. In: Proceedings of the IEEE/CVF Conference on Computer Vision and Pattern Recognition. pp. 12444–12453 (2022)
48. Meng, Q., Yan, S., Xiao, M., Wang, Y., Lin, Z., Luo, Z.Q.: Training much deeper spiking neural networks with a small number of time-steps. *Neural Networks* **153**, 254–268 (2022)
49. Merolla, P.A., Arthur, J.V., Alvarez-Icaza, R., Cassidy, A.S., Sawada, J., Akopyan, F., Jackson, B.L., Imam, N., Guo, C., Nakamura, Y.: A million spiking-neuron integrated circuit with a scalable communication network and interface. *Science* **345**(6197), 668–673 (2014)
50. Merolla, P.A., Arthur, J.V., Alvarez-Icaza, R., Cassidy, A.S., Sawada, J., Akopyan, F., Jackson, B.L., Imam, N., Guo, C., Nakamura, Y., et al.: A million spiking-neuron integrated circuit with a scalable communication network and interface. *Science* **345**(6197), 668–673 (2014)
51. Miao, S., Chen, G., Ning, X., Zi, Y., Ren, K., Bing, Z., Knoll, A.: Neuromorphic vision datasets for pedestrian detection, action recognition, and fall detection. *Frontiers in neuro-robotics* **13**, 38 (2019)
52. Orchard, G., Jayawant, A., Cohen, G.K., Thakor, N.: Converting Static Image Datasets to Spiking Neuromorphic Datasets Using Saccades. *Frontiers in Neuroscience* **9** (2015)
53. Panda, P., Aketi, S.A., Roy, K.: Toward scalable, efficient, and accurate deep spiking neural networks with backward residual connections, stochastic softmax, and hybridization. *Frontiers in Neuroscience* **14**, 535502 (2020)
54. Park, N., Kim, S.: How do vision transformers work? arXiv preprint arXiv:2202.06709 (2022)

55. Paszke, A., Gross, S., Massa, F., Lerer, A., Bradbury, J., Chanan, G., Killeen, T., Lin, Z., Gimelshein, N., Antiga, L., et al.: Pytorch: An imperative style, high-performance deep learning library. *Advances in neural information processing systems* **32** (2019)
56. Pei, J., Deng, L., Song, S., Zhao, M., Zhang, Y., Wu, S., Wang, G., Zou, Z., Wu, Z., He, W., et al.: Towards artificial general intelligence with hybrid tianjic chip architecture. *Nature* **572**(7767), 106–111 (2019)
57. Rao, A., Plank, P., Wild, A., Maass, W.: A long short-term memory for ai applications in spike-based neuromorphic hardware. *Nature Machine Intelligence* **4**(5), 467–479 (2022)
58. Rathi, N., Chakraborty, I., Kosta, A., Sengupta, A., Ankit, A., Panda, P., Roy, K.: Exploring neuromorphic computing based on spiking neural networks: Algorithms to hardware. *ACM Computing Surveys* **55**(12), 1–49 (2023)
59. Rathi, N., Srinivasan, G., Panda, P., Roy, K.: Enabling deep spiking neural networks with hybrid conversion and spike timing dependent backpropagation. *arXiv preprint arXiv:2005.01807* (2020)
60. Roy, K., Jaiswal, A., Panda, P.: Towards spike-based machine intelligence with neuromorphic computing. *Nature* **575**(7784), 607–617 (2019)
61. Schuman, C.D., Kulkarni, S.R., Parsa, M., Mitchell, J.P., Kay, B., et al.: Opportunities for neuromorphic computing algorithms and applications. *Nature Computational Science* **2**(1), 10–19 (2022)
62. Selvaraju, R.R., Cogswell, M., Das, A., Vedantam, R., Parikh, D., Batra, D.: Grad-cam: Visual explanations from deep networks via gradient-based localization. In: *Proceedings of the IEEE international conference on computer vision*. pp. 618–626 (2017)
63. Shen, S., Zhao, D., Shen, G., Zeng, Y.: Tim: An efficient temporal interaction module for spiking transformer. *arXiv preprint arXiv:2401.11687* (2024)
64. Si, C., Yu, W., Zhou, P., Zhou, Y., Wang, X., Yan, S.: Inception transformer. *Advances in Neural Information Processing Systems* **35**, 23495–23509 (2022)
65. Sironi, A., Brambilla, M., Bourdis, N., Lagorce, X., Benosman, R.: HATS: Histograms of Averaged Time Surfaces for Robust Event-Based Object Classification. In: *Proceedings of the IEEE Conference on Computer Vision and Pattern Recognition*. pp. 1731–1740 (2018)
66. Stewart, K.M., Neftci, E.O.: Meta-learning spiking neural networks with surrogate gradient descent. *Neuromorphic Computing and Engineering* **2**(4), 044002 (2022)
67. Su, Q., Chou, Y., Hu, Y., Li, J., Mei, S., Zhang, Z., Li, G.: Deep directly-trained spiking neural networks for object detection. In: *Proceedings of the IEEE/CVF International Conference on Computer Vision*. pp. 6555–6565 (2023)
68. Tripura, T., Chakraborty, S.: Wavelet neural operator for solving parametric partial differential equations in computational mechanics problems. *Computer Methods in Applied Mechanics and Engineering* **404**, 115783 (2023)
69. Vaswani, A., Shazeer, N., Parmar, N., Uszkoreit, J., Jones, L., Gomez, A.N., Kaiser, A., Polosukhin, I.: Attention is all you need. *Advances in neural information processing systems* **30** (2017)
70. Viale, A., Marchisio, A., Martina, M., Masera, G., Shafique, M.: Carsnn: An efficient spiking neural network for event-based autonomous cars on the loihi neuromorphic research processor. In: *2021 International Joint Conference on Neural Networks (IJCNN)*. pp. 1–10. IEEE (2021)
71. Wang, Z., Fang, Y., Cao, J., Zhang, Q., Wang, Z., Xu, R.: Masked spiking transformer. In: *Proceedings of the IEEE/CVF International Conference on Computer Vision*. pp. 1761–1771 (2023)
72. Yang, Z., Wu, Y., Wang, G., Yang, Y., Li, G., Deng, L., Zhu, J., Shi, L.: DashNet: A hybrid artificial and spiking neural network for high-speed object tracking. *arXiv preprint arXiv:1909.12942* (2019)

73. Yao, M., Gao, H., Zhao, G., Wang, D., Lin, Y., Yang, Z., Li, G.: Temporal-wise attention spiking neural networks for event streams classification. In: Proceedings of the IEEE/CVF International Conference on Computer Vision. pp. 10221–10230 (2021)
74. Yao, M., Gao, H., Zhao, G., Wang, D., Lin, Y., Yang, Z., Li, G.: Temporal-wise attention spiking neural networks for event streams classification. In: Proceedings of the IEEE/CVF International Conference on Computer Vision. pp. 10221–10230 (2021)
75. Yao, M., Hu, J., Zhou, Z., Yuan, L., Tian, Y., Xu, B., Li, G.: Spike-driven transformer. arXiv preprint arXiv:2307.01694 (2023)
76. Yao, M., Zhao, G., Zhang, H., Hu, Y., Deng, L., Tian, Y., Xu, B., Li, G.: Attention spiking neural networks. *IEEE transactions on pattern analysis and machine intelligence* (2023)
77. Yao, T., Pan, Y., Li, Y., Ngo, C.W., Mei, T.: Wave-vit: Unifying wavelet and transformers for visual representation learning. In: European Conference on Computer Vision. pp. 328–345. Springer (2022)
78. Yao, X., Li, F., Mo, Z., Cheng, J.: Glif: A unified gated leaky integrate-and-fire neuron for spiking neural networks. *Advances in Neural Information Processing Systems* **35**, 32160–32171 (2022)
79. Ye, C., Kornijcuk, V., Yoo, D., Kim, J., Jeong, D.S.: Lacera: Layer-centric event-routing architecture. *Neurocomputing* **520**, 46–59 (2023)
80. Zhang, J., Dong, B., Zhang, H., Ding, J., Heide, F., Yin, B., Yang, X.: Spiking Transformers for Event-Based Single Object Tracking. In: Proceedings of the IEEE/CVF Conference on Computer Vision and Pattern Recognition. pp. 8801–8810 (2022)
81. Zheng, H., Wu, Y., Deng, L., Hu, Y., Li, G.: Going deeper with directly-trained larger spiking neural networks. In: Proceedings of the AAAI Conference on Artificial Intelligence. vol. 35, pp. 11062–11070 (2021)
82. Zheng, H., Wu, Y., Deng, L., Hu, Y., Li, G.: Going deeper with directly-trained larger spiking neural networks. In: Proceedings of the AAAI conference on artificial intelligence. vol. 35, pp. 11062–11070 (2021)
83. Zhou, C., Yu, L., Zhou, Z., Zhang, H., Ma, Z., Zhou, H., Tian, Y.: Spikingformer: Spike-driven residual learning for transformer-based spiking neural network. arXiv preprint arXiv:2304.11954 (2023)
84. Zhou, Z., Zhu, Y., He, C., Wang, Y., Yan, S., Tian, Y., Yuan, L.: Spikformer: When spiking neural network meets transformer. arXiv preprint arXiv:2209.15425 (2022)
85. Zhu, R.J., Zhao, Q., Zhang, T., Deng, H., Duan, Y., Zhang, M., Deng, L.J.: Tcja-snn: Temporal-channel joint attention for spiking neural networks. arXiv preprint arXiv:2206.10177 (2022)